A spatiotemporal transcriptomic network dynamically modulates stalk development in maize

Liang Le[1,2,†] (iD), Weijun Guo[1,†], Danyao Du[1,†], Xiaoyuan Zhang[1,†], Weixuan Wang[1], Jia Yu[1], Huan Wang[1], Hong Qiao[3,4], Chunyi Zhang[1,5,*] and Li Pu[1,2,*] (iD)

[1]*Biotechnology Research Institute, Chinese Academy of Agricultural Sciences, Beijing, China*

[2]*National Nanfan Research Institute (Sanya), Chinese Academy of Agricultural Sciences, Sanya, China*

[3]*Institute for Cellular and Molecular Biology, The University of Texas at Austin, Austin, TX, USA*

[4]*Department of Molecular Biosciences, The University of Texas at Austin, Austin, TX, USA*

[5]*Sanya Institute, Hainan Academy of Agricultural Sciences, Sanya, China*

Summary

Maize (*Zea mays*) is an important cereal crop with suitable stalk formation which is beneficial for acquiring an ideal agronomic trait to resist lodging and higher planting density. The elongation pattern of stalks arises from the variable growth of individual internodes driven by cell division and cell expansion comprising the maize stalk. However, the spatiotemporal dynamics and regulatory network of the maize stalk development and differentiation process remain unclear. Here, we report spatiotemporally resolved transcriptomes using all internodes of the whole stalks from developing maize at the elongation and maturation stages. We identified four distinct groups corresponding to four developmental zones and nine specific clusters with diverse spatiotemporal expression patterns among individual internodes of the stalk. Through weighted gene coexpression network analysis, we constructed transcriptional regulatory networks at a fine spatiotemporal resolution and uncovered key modules and candidate genes involved in internode maintenance, elongation, and division that determine stalk length and thickness in maize. Further CRISPR/Cas9-mediated knockout validated the function of a cytochrome P450 gene, *ZmD1*, in the regulation of stalk length and thickness as predicted by the WGCN. Collectively, these results provide insights into the high genetic complexity of stalk development and the potentially valuable resources with ideal stalk lengths and widths for genetic improvements in maize.

Introduction

Maize (*Zea mays*) is a major cereal crop and a model plant for exploring ideal agronomic traits for lodging resistance and the adverse effects of higher planting densities (Xiao *et al*., 2017). The plant height (PH) of mature maize largely results from stalk elongation (Avila *et al*., 2016). During maize growth, the stalk elongates in a sigmoidal pattern that arises from the variable growth rates of individual internodes comprising the maize stalk (Fournier and Andrieu, 2000). Many important biological processes may be involved in stalk elongation, including cell division, cell wall synthesis, and vascular bundle formation (Cui *et al*., 2012). Considering that maize PH primarily results from stalk elongation driven by cell division and cell expansion within the internodes, uncovering the dynamic transcriptome of individual internodes within the whole stalk and identifying new cell elongation-related regulators may be a solution for exploring ideal plant architecture. However, the regulatory network that controls maize stalk development is still not well understood.

To better understand the regulation of maize stalk development, several recent studies have used next-generation sequencing (NGS) technologies to survey transcriptomic differences among maize stalk cell types and developmental stages (Stelpflug *et al*., 2016; Yu *et al*., 2015). Stelpflug *et al*. obtained B73 developmental gene atlas data of 79 tissues, including eight stalk tissues, and found that the transcriptomes of the fourth internode at the V9 stage had a strong correlation with the transcriptomes of the shoot tip (Stelpflug *et al*., 2016). Hoopes et al. reanalyzed Stelpflug's 79-tissue B73 transcriptome dataset with the updated AGPv4 assembly and annotation of the reference accession B73 to identify internode-specific genes that were enriched for 'regulation of gene expression' (GO:0010468) (Hoopes *et al*., 2019). The length of the internode below the seventh internode did not change significantly, but the length of the ninth internode continuously increased after the ninth leaf expanded (Peng *et al*., 2019). Nevertheless, no comprehensive comparisons of internode-specific transcriptomes along maize stalks have been performed.

Maize stalk lodging has a highly adverse effect on yield, quality, and mechanized harvesting and is one of the main problems to be solved urgently in modern maize production and breeding. The thickness of the stalk is closely related to stalk strength, which is an important contributor to stalk lodging resistance (Peiffer *et al*., 2013). Stalk cell development plays a general role in not only the control of cell length but also cell width in maize. For example, overexpression of the *Reducing Plant Height 1* (*ZmRPH1*) gene, which encodes a QWRF homologous microtubule-associated protein, controls plant and ear height via reduced cell length but increases cell width in maize seedlings (Li *et al*., 2020b). Stalk thickness determined by cell width can

significantly enhance resistance to fracture (Jiao *et al.*, 2019; Kashiwagi *et al.*, 2006; Zuber *et al.*, 1999). Many genes that play vital roles in stalk elongation have been identified by studying PH mutants (maize GDB). In maize, mutants of the *Dwarf1* and *Dwarf3* genes that mediate gibberellic acid (GA) synthesis show dwarfism (Chen *et al.*, 2014; Winkler and Helentjaris, 1995). In addition, *Dwarf8* and *Dwarf9*, which regulate DELLA proteins of GA signal transduction pathways, have been genetically and phenotypically characterized in maize (Cassani *et al.*, 2009; Lawit *et al.*, 2010; Winkler and Freeling, 1994). These studies provided insight into the regulatory mechanisms underlying the development of stalk anatomy in maize. However, the spatiotemporal dynamics and regulation of the stalk development and differentiation process remain unclear.

In this study, we obtained 58 transcriptomes of individual internodes of maize stalks from the elongation stage (ES) and the maturation stage (MS) to elucidate the spatiotemporal gradient of culm development. In total, 13 964 genes with a high coefficient of variation (CV) were classed into four distinct zones and nine coexpression modules according to their expression patterns, which provided further insight into the spatiotemporal transitions in mRNA abundance of the four zones. The phenotype-specific network modules were identified by combining transcriptome data with stalk phenotype data through weighted gene coexpression network analysis (WGCNA). Many crucial cell elongation regulatory genes, including *Cytochrome P450 D1* (*ZmD1*) and *Brassinzole-resistant 1* (*ZmBZR1*), were identified as hub genes in the elongated stalk network. We validated that loss of *ZmD1* function resulted in a shorter stature and bulkier culm than the wild type (WT), corroborating the critical role of the *ZmD1* gene in maize stalk development. In summary, spatiotemporally resolved transcriptomes provide a valuable and credible resource for an enhanced understanding of stalk development and greater control for crop improvement.

Results

Dynamic transcriptomic analyses of individual internodes of stalks at the elongation and maturation stages in maize

To create inventories of dynamic gene expression patterns during the maize stalk elongation process, we selected all internodes of stalks at V14 (rapid growth, when the 14th leaf had unfurled) and R6 (maturity) stages, which represent ES and MS, respectively, for time-point transcriptome sequencing (Figure 1a). Two biological replicates, each of which consisted of pooled samples from at least three plants, were set up for all 29 groups corresponding to individual internodes at the ES (12 groups) and MS (17 groups). An average of ~72.8% of reads were uniquely mapped, and only the uniquely mapped reads were further employed to calculate the normalized gene expression level as fragments per kilobase of

transcript per million mapped (FPKM) reads. The numbers of expressed genes and respective expression levels in each sample type were based on the average FPKM reads of two biological replicates (Figure S1a). To decrease the influence of transcription noise, we defined a gene as expressed if its FPKM value was ≥1. The overall expression of genes in the MS samples was lower than that in the ES samples (Figure S1a).

To gain insight into the dynamic transcriptome of maize stalk development, we performed correlation analysis (Figure S1b), hierarchical clustering (Figure 1b), and principal component analysis (PCA) (Figure 1c). The transcriptomes of the upper stalks (the fifth to top internodes) at the ES were entirely different from those of the other stalks at the ES or MS (Figure 1b,c), which coincided with the elongation process occurring primarily in these stalks. PCA yielded three principal components (PCs) that collectively explained 94.54% of the total sample variance in the transcriptomic data. Through PCA and hierarchical clustering, these high-density internode transcriptomes could be generally divided into four groups, each corresponding to a specific spatiotemporal expression pattern, including the elongation partially complete zone (EPCZ, Zone I), the division zone (DZ, Zone II), the base zone (BZ, Zone III), and the mature zone (MZ, Zone IV) (Figure 1b,c).

High-temporal resolution transcriptomes were clustered into four zones corresponding to specific spatiotemporal expression patterns

Samples from bottom stalks containing internode 2 from aerial roots (ES_UGN2 and ES_UGN1) and internodes ES_1~4 formed the first cluster and represented the expression pattern around Zone I. The first zone with specifically expressed genes coincided with the fast elongation from the ES to MS, involving extensive physiological changes. For example, the *Zm00001d027938* gene, which encodes a hexosyltransferase, affects the cell wall development of elongated internodes by participating in the transition from primary cell wall to secondary cell wall synthesis (Peng *et al.*, 2019). *Zm00001d015845* (*ZmBzip28*) is a transcriptional activator involved in ER stress responses that activate brassinosteroid (BR) signalling pathway proteins and is required for stress acclimation and cell growth in *Arabidopsis* (Che *et al.*, 2010). *Zm00001d039453* (*ZmD1*) encodes a cytochrome P450 protein related to BR biosynthetic processes, sterol metabolic processes, and multicellular organism development (Kim *et al.*, 2005). *Zmhexosyltransferase*, *ZmBzip28*, and *ZmD1* were all highly expressed in Zone I but rapidly decreased from the fifth internode to the top of ES stalks (Figure 1d).

The samples from the fifth to top internodes at ES formed a second cluster and represented the expression pattern of Zone II. The expansion of this zone involving a subset of genes plays an essential role in the final PH. For instance, the overexpression of *Zm00001d028073* (*ZmRPH1*), which encodes a QWRF

Figure 1 Transcriptomic analyses of internodes of the maize stalk at the elongation and maturation stages. (a) Morphological characterization (left panel) and growth pattern (right panel) of maize at the elongation stage (ES) and maturation stage (MS). UGN2_ES and UGN1_ES represent the second and last internodes underground at the elongation stage, respectively. N1_ES to N9_ES represent the first to ninth internodes of fast-growing maize. MS represents mature maize. Cluster dendrogram (b) and PCA (c) of the transcriptomes of all 29 internode groups. (d–g) The selected marker genes were mainly expressed in the zones with gene expression patterns I (d), II (e), III (f), and IV (g). The time points belonging to the zone with gene expression patterns I, II, III, and IV are shown in light blue, yellow, deep yellow, and light green, respectively. BZ, base zone; DZ, division zone; EPCZ, elongation partially complete zone; MZ, mature zone.
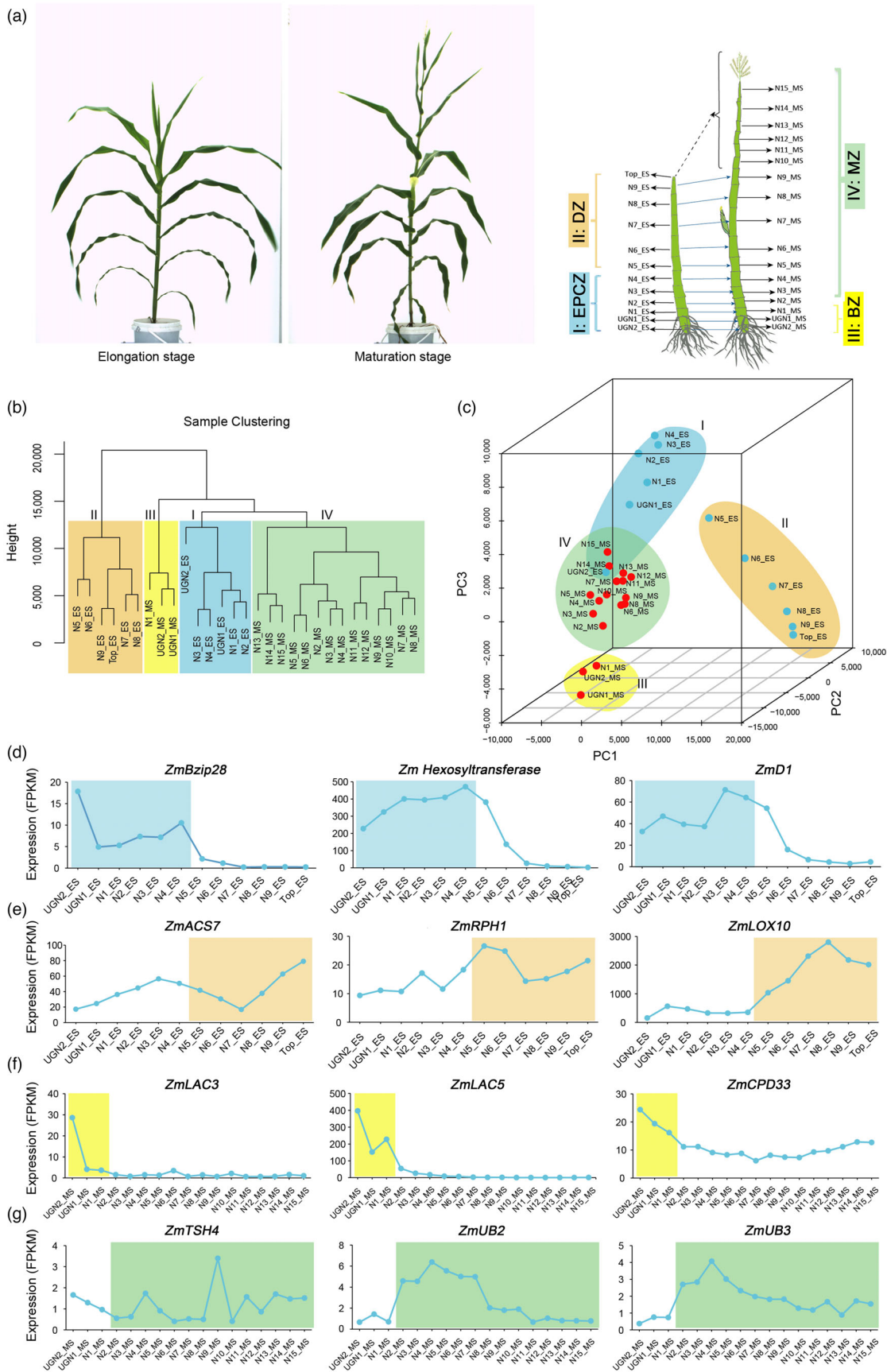
homologue protein, lowered PH and ear height by reducing the length of all internodes and increased lodging resistance without significantly reducing maize yield (Li et al., 2020b). The mutant of the *Zm00001d026060* (*ZmACS7*) gene which encodes 1-aminocyclopropane-1-carboxylate synthase 7 in the ethylene biosynthesis of maize and confers the phenotypes of the *Semidwarf3* (*Sdw3*) mutant exhibits a shorter stature and larger leaf angle than the WT (Li et al., 2020a). As a plant lipoxygenase gene, *Zm00001d053675* (*ZmLOX10*) may be involved in many diverse aspects of plant physiology, including growth and development, pest resistance, and wound response (Christensen et al., 2013). Three genes *ZmRPH1*, *ZmACS7*, *and ZmLox10* were extremely highly expressed in the upper section of the ES stalk (Figure 1e), indicating their essential effect on the regulation of cell division and stalk development. The samples collected under the second internode at the MS (MS_UGN1, MS_UGN2, and MS_N1) fell into the third cluster and represented the expression pattern of Zone III. *Zm00001d025564* (*ZmLAC3*) *and Zm00001d033710* (*ZmLAC5*), which are two target genes of miRNA528, have been proven to affect lignin synthesis and ultimately weaken lodging resistance in maize (Sun et al., 2018). The *Carbohydrate Partitioning Defective33* (*Zm00001d011239*, *ZmCPD33*) encodes a protein containing multiple C2 domains and transmembrane regions which function to promote sucrose transport from leaves into sieve elements (Tran et al., 2019). In the MS stalk, the *ZmLAC3*, *ZmLAC5*, and *ZmCPD33* genes were highly expressed in Zone III, while decreased or not expressed in the upper internodes, implying that the highly expressed genes in this zone might be associated with lodging resistance and the transport of necessary nutrients or substances (Figure 1f).

The fourth cluster was from the second internode to the tassel at MS, which corresponds to the expression pattern of Zone IV. *Tasselsheath4* (*ZmTSH4*, *Zm00001d020941*), *Unbranched2* (*ZmUB2*, *Zm00001d031451*), *and ZmUB3* (*Zm00001d052890*), also called *Squamosa-Promoter Binding Protein 6* (*ZmSBP6*), *ZmSBP8*, and *ZmSBP30*, respectively, were direct targets of miR156s, showing complementarity to the sequences of mature *zma-miR156s* (Chuck et al., 2010, 2014). It was reported that single or double mutants of *ZmUB2* and *ZmUB3* did not change PH, whereas mutation of *ZmTSH4* resulted in dwarf maize plants with abundant tillers (Chuck et al., 2014). *ZmUB2* and *ZmUB3* were highly expressed in Zone IV, which is consistent with the zone maintaining tassel function (Figure 1g). In summary, our results demonstrated the transcriptional dynamics of stalk elongation and maturation with four distinct spatiotemporal groups corresponding to four different zones, each of which showed additional internal dynamic features. These data reveal a previously undescribed dissection of the transcriptional hierarchies and mechanistic regulation promoting fast stalk growth in maize.

Nine specific gene expression patterns characterize stalk elongation and growth in maize at different developmental stages

Global hierarchical clustering and PCA graphically display the four zones of maize stalk at the ES and MS. To further provide insights into the functional transitions during stalk development, the expression patterns of all 13 964 genes with a high CV (>0.4) were clustered into nine coexpression clusters using the fuzzy c-means clustering algorithm (Figure 2a, Table S1). We performed Gene Ontology (GO) enrichment analysis and reduced dimensionality to assign these genes to functional categories for these clusters (Figure 2c–k). In the maize stalk, Clusters 2 and 7 exhibited 1860 and 1071 genes with high CVs in Zone I, respectively (Figure 2a,b). The 1860 genes might be involved in metabolic processes, photosynthesis, and the generation of precursor metabolites and energy (Figure 2d). The 1071 genes that encode enzymes for DNA-templated transcriptional activation were enriched in Cluster 7 (Figure 2i). These biological processes are consistent with the functions of cells undergoing rapid elongation in Zone I.

Clusters 1, 5, and 9 exhibited peak gene expression in the division zone (Zone II), which is the zone containing the most dynamically changed genes. Cluster 1 contained 1826 genes associated with metabolic processes, DNA-binding TF activity, and defence responses. These genes might be involved in rapid cell proliferation and differentiation because they are mainly expressed at ES_N8, ES_N9, and ES_Top (Figure 2c). Cluster 5 included 901 genes associated with cell wall organization or biogenesis, cellular oxidant detoxification, external encapsulating structure organization, and polysaccharide metabolic process at ES_N5 and ES_N6 (Figure 2g). The 1086 genes in Cluster 9 were intensely expressed in Zone II at the ES and represented by genes corresponding to cell wall biogenesis, auxin transport, and response to auxin, which shared some similar GO terms with Cluster 5 (Figure 2k). Interestingly, several of these biological functions are also overrepresented in the root tip, such as cell wall organization or biogenesis and transcription activity (Li et al., 2014; Stelpflug et al., 2016). Genes with peak expression in Zone II are represented by three clusters (Clusters 1, 5, and 9) involved in processes required for cell elongation, such as polysaccharide metabolic processes, cell wall organization and biogenesis, and auxin transport. This result is consistent with processes associated with cell wall elongation, deposition, and reorganization during auxin-mediated stalk elongation and differentiation in Zone II.

Cluster 6 displayed 1068 genes that were highly expressed in Zone III. These genes are mainly involved in cytoskeletal organization, cellular component organization or biogenesis, movement of a cell or subcellular components, and microtubule-based processes (Figure 2h). Clusters 4 and 8 revealed peak gene expression in Zone IV. A total of 1887 genes in Cluster 8 encoded ribosome assembly, sterol biosynthetic process, microtubule-based process, and cell, or subcellular component movement, sharing some similar GO terms with Cluster 6 (Figure 2j). Additionally, we identified 2275 genes in Cluster 4 that were gradually upregulated from MS_N9 to MS_N15 and involved in the nuclear division, DNA-dependent DNA replication, and regulation of the cell cycle, indicating the essential impact of these genes on tassel development (Figure 2f).

Figure 2 Spatiotemporal gene expression pattern of maize stalk and functional enrichment analysis. (a) Fuzzy c-means clustering shows the dynamic expression profile of individual internodes of maize stalks at the elongation and maturation stages. Nine clusters were identified along all internode and the two developmental stages from 13 964 genes with a high coefficient of variation. (b) Pie chart showing the proportion of nine clusters. (c–k) Functional category enrichment (modified from Mapan bins) of the nine fuzzy c-means clusters, namely Cluster 1 (c), Cluster 2 (d), Cluster 3 (e), Cluster 4 (f), Cluster 5 (g), Cluster 6 (h), Cluster 7 (i), Cluster 8 (j), and Cluster 9 (k). C1–C9 represent Clusters 1–9.
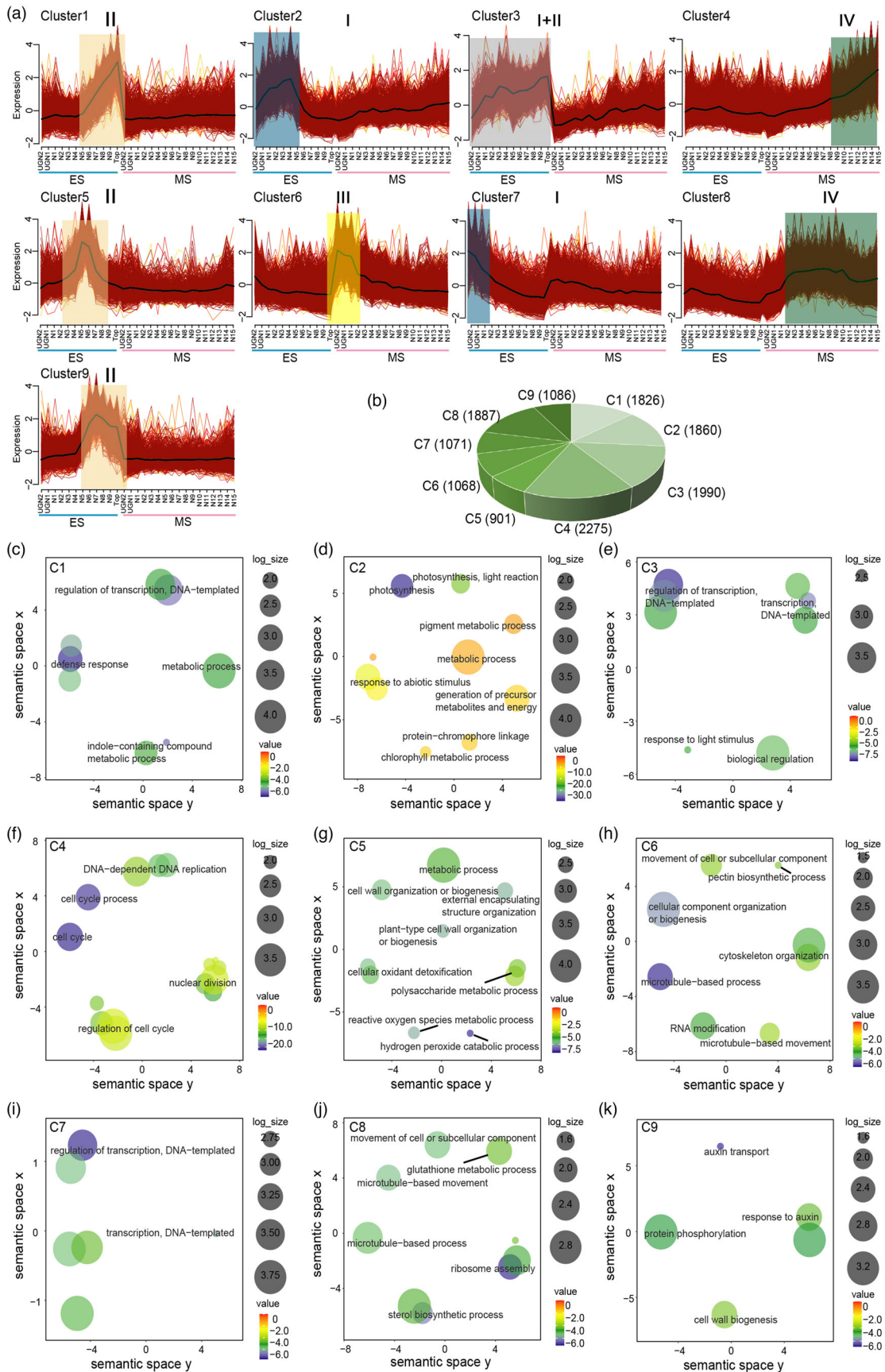
We also found that 1990 genes in Cluster 3 were predominantly expressed in the whole stalk at the ES, indicating some common functional processes in the ES stalk. For instance, genes encoding enzymes involved in the regulation of DNA-templated transcription, response to light stimulus, and biological regulation displayed continuous expression in Zones I and II (Figure 2e). Together, these results revealed the major biochemical shifts among individual internodes of whole stalks at the ES and MS that are triggered partly by vastly dynamic and spatiotemporal transitions in mRNA abundance.

Dynamic changes in hormone-related and TF genes essential for stalk elongation and growth in maize

Since many PH-related genes that have been reported in maize are transcription factors (TFs) or involved in hormone signalling (Chen *et al*., 2014; Chuck *et al*., 2014; Lu *et al*., 2020), we further investigated the role of hormones and TFs in the stalk developmental transition. A total of 375 expressed genes from the spatiotemporal transcriptome profiling dataset were identified that might participate in the action of eight major plant hormones, abscisic acid (ABA), auxin, BR, cytokinin (CK), ethylene, GA, jasmonic acid (JA), and salicylic acid (SA) (Figure 3). Hormone-related genes in each class were divided into three types, namely synthesis-degradation (C1), signal transduction (C2), and induced-regulated responsive-activated (C3) as previously reported (Yu *et al*., 2015) (Figure 3). We found that most of the hormone-related genes were expressed in a specific spatiotemporal manner (Figure 3, dotted rectangles). For example, auxin-induced regulated responsive-activated genes (C3) were specifically expressed in Zone I (Figure 3d), including *Auxin-Induced in Root Culture Protein 12* (*AIR12*), *Aluminium-Induced Protein* (*AILP1*), and the maize ortholog of *GH3.6* (*Indole-3-Acetic Acid-Amido Synthetase*), which function in shoot and hypocotyl cell elongation (Table S2). ABA-, GA-, BR-, ethylene-, and JA-related synthesis degradation genes (C1) were specifically expressed in the mature maize stalks (Figure 3a, b, e–g, Table S2).

Additionally, many C1 genes were highly expressed in the division zone (Zone II) at the ES and continued to be expressed at the MS (Figure 3), including BR-, JA-, and SA-related C1 genes (Figure 3e, g, and h), such as *DWF1* (*Dwarf1*) (BR), *DWF7* (BR), *SMT2* (*Sterol Methyltransferases 2*) (BR), and *LOX1* (*Lipoxygenase 1*) (JA), in accordance with their crucial significance in cell elongation or vascular differentiation (Table S2). Manipulating BR levels by regulating the gene expression of *DWF1*, *DWF4*, or *DWF7* effectively improves maize agronomic traits, including enlarging leaf area, increasing PH and photosynthesis, delaying leaf senescence or improving grain yields (Choe *et al*., 1999; Knoch *et al*., 2018; Liu *et al*., 2020).

The C2 genes relevant to hormone signal transduction were widely expressed in the whole stalks at both the ES and MS (Figure 3). CK-related C2 genes included *CK Oxidase 5* (*CKX5*) and *CK Oxidase 7* (*CKX7*), with peak expression in the maturation stalk, modulating CK levels to maintain plant growth (Table S2) (Brugiere *et al*., 2003). The maize ortholog of *Ga Requiring 3*

(*GA3*), which controls the elongation of the vegetative shoot and PH by regulating gibberellin levels, was extremely highly expressed in the mature stalk (Table S2). The auxin-related C2 gene with a maize ortholog of *Pin-Formed 1* (*PIN1*) was specifically expressed in the upper part of the mature maize stalk, which was consistent with its function as a component of the auxin efflux carrier to sustain tassel development (Table S2) (Chen *et al*., 2012). Briefly, our results showed that most of the hormone-related genes are specifically expressed in a specific manner in different zones and at different stages, suggesting that the hormone regulation of stalk elongation is a considerably complicated process.

The dynamics of TF expression during cell elongation and differentiation along the maize stalk axis were especially well-resolved in our transcriptome data. We classified 2165 expressed TF genes into four groups, including hormone-related, growth and development, response to stress-genes, and others (Figure S2). Interestingly, the numbers of LFY and YABBY family members gradually increased from the bottom to the top of the stalks at the ES (Figure S2b). YABBY family genes, including *yabby3*, *yabby9*, and *yabby15*, had the highest expression levels in the top tissue of the elongation stalk (Table S3), which was in line with their function in apical cell fate specification (Ku *et al*., 2012).

Identification of differentially expressed genes associated with internode maintenance, elongation, and division

To understand how factors control stalk development and identify novel internode regulators, five representative internodes from the four different developmental zones were selected to perform a comparative analysis of differential gene expression (Figure 4a). The length of N1 from the ES to MS remained almost unchanged, while that of N7 was significantly increased, indicating rapid elongation in the seventh internode from the ES to MS (Figure 4b, S3). The ES_Top contained the vegetative shoot apical meristem and formed the top six internodes in the MS through the division process. Thus, we compared the transcriptomes of ES_Top with those of ES_N1 in the same stalk to determine the specific gene expression pattern in the division zone. The comparison between MS_N7 and MS_N1 would indicate the distinction of the internodes in the MS stalk. Genes were considered differentially expressed genes (DEGs) when the *P* value, adjusted for multiple hypothesis testing, was ≤0.05 (Zhou *et al*., 2019). Interestingly, approximately 3000 DEGs were identified in the ES_Top versus ES_N1 and MS_N7 versus ES_N7 comparisons, indicating that these DEGs might be involved in the division and elongation process in maize. However, only half of the DEGs involved in the division process were identified in the MS_N7 versus MS_N1 (1222 DEGs) and MS_N1 versus ES_N1 (1526 DEGs) comparisons (Figure 4c). Although these internodes representing the division and elongation processes were different, the number of overlapping DEGs between the two processes were 1577, accounting for 51.6% (1577/3056) and 51.5% (1577/3062) of the DEGs in the division and elongation processes,

Figure 3 Dynamic expression patterns of hormone-related genes among individual internodes of the maize stalk at the elongation and maturation stages. Normalized expression levels of genes related to (a) abscisic acid (ABA), (b) gibberellic acid (GA), (c) brassinolide (BR), (d) auxin, (e) cytokinin (CK), (f) ethylene, (g) jasmonic acid (JA), and (h) salicylic acid (SA) are shown. For each hormone, its related genes are divided into three functional categories: (C1) synthesis-degradation, (C2) signal transduction, and (C3) induced-regulated-responsive-activated.

(a) ABA (b) GA (c) CK (d) Auxin (e) BR (f) ethylene (g) JA (h) SA

C1. Synthesis-degradation

C2. Signal transduction

C3. Induced-regulated responsive-activated
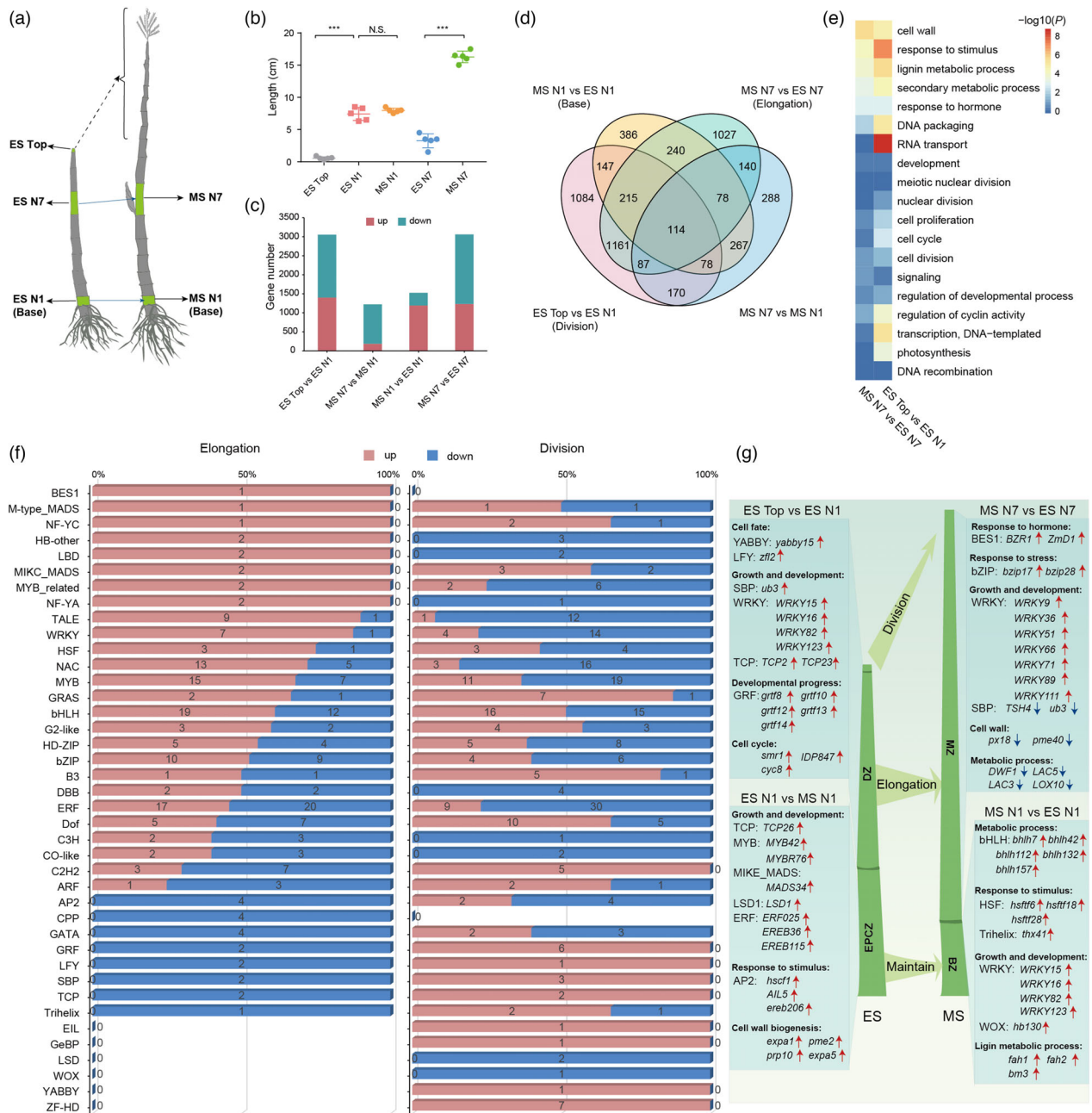
Figure 4 Dynamic inventories of differentially expressed genes (DEGs) orchestrate internode growth and development. (a) Representative internodes of four developmental zones. (b) The length of these representative internodes. (c) The number of DEGs among these representative internodes. (d) The Venn diagram shows the overlap of DEGs among these representative internodes. (e, f) Overview of DEGs (f) and transcription factors (TFs, f) in the division zones and elongation zones. Elongation represents the comparison between MS_N7 and ES_N7, and division represents the comparison between ES_Top and ES_N1. (g) Distribution of the representative TF families and other genes differentially expressed in the four zones.

respectively (Figure 4d). GO analysis of DEGs between ES_Top and ES_N1 showed that DNA transcription, RNA transport, cell cycle and proliferation, and nuclear division were involved in the division process, but cell wall, response to stimulus, and secondary metabolic process were involved in the elongation process (Figures 4e, S3). As shown in Figure S2, the numbers of *LFY* and *YABBY* family members specifically increased at the top of the ES stalk. Compared to those in the ES_N1 group, the *LFY* and *YABBY* genes determining cell fate were upregulated in the ES_Top stalk, including *YABBY15* and *ZFL2* (Figure 4f,g),

suggesting that they may play important roles in regulating elongation in a spatially explicit manner. We found that the expression levels of growth-regulating factors (GRFs) that were plant-specific TFs with vital roles in stem and leaf development were also increased in the ES_Top stalk (Kim and Lee, 2006), such as *GRTF8, GRTF10, GRTF12, GRTF13, and GRTF14* (Figure 4f,g). Furthermore, we found that the cell cycle genes that played important roles in the division process to determine stalk length were significantly increased in the ES_Top, such as *SMR1, IDP847,* and *CYC8* (Figure 4g).

However, GO terms of DEGs between MS_N7 and ES_N7 were mainly enriched in response to hormone, response to stress, growth and development, cell wall, and metabolic process (Figure S3). Notably, many plant architecture-related genes (*TSH4*, *ub3*, *DWF1*, *LAC3*, *LAC5*, and *LOX10*) and cell wall-related genes showed downregulated expression patterns in MS_N7 compared with ES_N7, indicating that these genes may play major roles in regulating the elongation process of the seventh internode at the early stage, which is required for fast growth in maize. In addition, members of the BES1, M-type_MADS, NF-YC, homeobox domain (HB)-other, lateral organ boundaries domain (LBD), and three amino acid loop extension (TALE) families of transcriptional regulators were also highly expressed in the MS_N7 where they probably have diverse functions in the determination of stalk cell number and cell size (Mei *et al.*, 2021) (Figure 4f,g).

It has been reported that the length of the base internode does not obviously differ during the maturation process, but the levels of the cell wall components cellulose, lignin, and glucuronoarabinoxylan (GAX) are dynamic in different internodes at different stages (Zhang *et al.*, 2014b). Indeed, we found that the length of the first internode did not change in the ES and MS (Figure 4b). Some participants of the lignin metabolic process including *FAH1*, *FAH2*, and *BM3* were highly expressed, but cell wall biogenesis-related genes (*EXPA1*, *EXPA5*, *PME2*, and *PRP10*) were downregulated in MS_N1 compared with ES_N1 (Figure 4g). Together, these results revealed a number of key genes involved in the transcriptional regulation of major stalk developmental events, division, elongation, and maintenance, thus modulating normal maize growth.

WGCNA identifies interrelated functional modules and hub genes

To reveal dynamic patterns and identify the transcriptional regulatory networks for stalk elongation in maize, we conducted WGCNA based on pairwise correlations between gene modules and the quantified physiological traits (length, diameter, perimeter, and weight) in the elongated stalks (Figure 5). The scale independence and mean connectivity were first computed at different thresholds (Figure 5a). With a scale independence >0.85 and connectivity <100 as the criteria, a soft threshold power of 4 was selected to classify coexpression modules. A cluster dendrogram was created based on the dissimilarity of the topological overlap matrix (Figure 5b). A total of 25 modules (labelled by different colours) were constituted by the tree branches, in which each leaf was one gene (Figure 5b). The module eigengene (ME), which represented the expression level of all genes in the module, was employed to identify significant correlations between modules and the phenotypes of maize stalks. The length and weight of intermediate nodes N2~N5 were greater than those of other nodes at the ES (Figure S4). However, the diameter and perimeter gradually increased and then rapidly decreased from bottom to top in maize stalks at ES (Figure S4). Our analysis focused on identified modules with significant module-trait correlations ($P < 0.001$) and contrasting expression patterns between genotypes (Figure 5c). The green module comprised 834 genes with the most significant correlation to internode length ($r = 0.87$; $P = 3 \times 10^{-4}$) and weight ($r = 0.93$; $P = 1 \times 10^{-5}$) (Figure 5c). To validate the relationship between the green module and phenotypes, we constructed a correlation scatterplot between the expression of 834 genes in the green module and the length, weight, diameter, and perimeter of each

internode (Figure 5d). Gene expression in the green module was notably correlated with internode length ($r = 0.67$; $P = 9.3 \times 10^{-110}$), weight ($r = 0.83$; $P = 1 \times 10^{-200}$), diameter ($r = 0.62$; $P = 9.9 \times 10^{-90}$), and perimeter ($r = 0.64$; $P = 2.7 \times 10^{-97}$) (Figure 5d).

Since internode length and weight might be affected by cell elongation, the 834 genes in the green module were further analysed for key biological processes and hub genes in relation to stalk elongation. The heatmap indicated that the expression pattern of the green module genes was similar to that of cluster 2 because the genes were exceedingly expressed in N1-4_ES (Figures 2a and 5e). The genes in the green module were involved in the regulation of hormone levels, signal transduction, response to hormones, and endogenous stimuli (Figure 5f), which demonstrated the indispensable role of hormones in stalk elongation and growth. The hub gene network of the green module was constructed by Cytoscape using a weight cutoff (>0.4), in which 7 hormone-related genes (green cycle) showed more connections, including 2 cytochrome P450 family genes (*ZmCYP87A2/Zm00001d013720* and *ZmD1/Zm00001d0139453*), 4 auxin-related genes (auxin-responsive protein SAUR61/*Zm00001d006274*, *Zm00001d006279*, *Zm00001d006282*, and *ZmAUX2/Zm00001d006283*), and 1 histone acetyltransferase (*Zmhagtf30/Zm00001d038491*) (Figure S5).

Interestingly, we found that the turquoise module that comprised 6549 genes was exceedingly negatively correlated with diameter ($r = -0.95$; $P = 3 \times 10^{-6}$) and perimeter ($r = -0.98$; $P = 5 \times 10^{-8}$) (Figure 5c). The expression trend of the turquoise module genes gradually increased from bottom to top with elongation of the maize stalk (Figure S6a), which indicated a similar expression pattern as Cluster 1 (Figure 2a). Gene expression in the turquoise module was extremely negatively correlated with the internode perimeter ($r = 0.95$; $P = 9.3 \times 10^{-200}$), diameter ($r = 0.93$; $P = 1 \times 10^{-200}$), weight ($r = 0.7$; $P = 1 \times 10^{-200}$), and perimeter ($r = 0.55$; $P = 1 \times 10^{-200}$) (Figure S6b). The genes in this module were mainly associated with protein binding and DNA binding (Figure S6c).

Besides the genes in the green module, 852 genes in the yellow module also showed a significant correlation to the internode phenotypes (Figures 5c and S7a). GO analysis showed that these genes were mainly involved in the regulation of ion transport, protein phosphorylation, and DNA transcription (Figure S7b). The expression trend of some key genes gradually decreased from bottom to top with elongation of the maize stalk, such as *Zm00001d050079* (Figure S7c). In *Arabidopsis*, *GLUTAMINE DUMPER 5* (*GUD5*), the ortholog of *Zm00001d050079* gene, encodes a probable subunit of an amino acid transporter involved in the regulation of the amino acid metabolism. Overexpression of *GUD5* leads to free amino acid levels accumulation and plant size decrease in *Arabidopsis* (Ma *et al.*, 2014; Pratelli *et al.*, 2010). Therefore, *GUD5* may be a novel candidate gene for stalk development in maize. Briefly, the green, turquoise as well as yellow module provide novel genes for cell length, cell width, and internode development genes during the elongation of the stalk, thereby influencing the length and thickness of the mature stalk.

Identification and validation of new genes associated with stalk elongation in maize

The expression of 7 hormone-related genes was obviously correlated with internode length ($r > 0.6$), weight ($r > 0.65$),

diameter ($r > 0.55$), and perimeter ($r > 0.45$), especially that of *Zm00001d039453* (*ZmD1*) (Figure 6a). The correlation coefficients between *ZmD1* expression and the four stalk phenotypes were higher than 0.75 (Figure 6a). The *ZmD1* is involved in distinct BR biosynthetic pathways and most likely participates in the oxidative C-3 epimerization of BRs (Kim *et al.*, 2005; Ren *et al.*, 2020; Tang *et al.*, 2010). Impressively, the expression of the BR-resistant 1 gene (*ZmBZR1/Zm00001d046305*) belonging to the turquoise module was negatively correlated with diameter and perimeter ($r < -0.75$) (Figure S8a–d). Intriguingly, the expression trends of *ZmD1* and *ZmBZR1* were complementary in maize stalks at the ES and MS (Figure S8e).

Therefore, we predict that *ZmD1* could be a key candidate gene for modulating cell length and width. As a cytochrome P450 family member, *ZmD1* was found to be widely expressed in various tissues, including almost all internodes, pollen, filaments, leaves, embryos, endosperm, and grains (Figure 6b–d). Nevertheless, the ZmD1 protein fused with GFP colocalized in the nucleus but dispersed in the periphery of the cell nucleus when the nuclear localization signal of the *ZmD1* gene was eliminated (Figure 6e). To further analyse the function of the *ZmD1* gene in maize stalk development, we generated two independent CRISPR/Cas9-mediated loss-of-function mutants (named *zmd1-1* and *zmd1-2*) (Figure S9a). The decrease in *ZmD1* gene expression was detected by qPCR (Figure S9b,c). We then measured PH and the length of all the internodes in mature maize stalks. The *zmd1* mutants resulted in shorter PHs and ear height (EH), and reduced internode lengths, especially the fifth-tenth internodes (Figure 7a–d). Conversely, the internode width was significantly increased, especially in the first to seventh internodes (Figure 7e, f). Reduced internode epidermal and parenchyma cell heights and increased cell widths in longitudinal sections were observed in *zmd1* mutants compared with the WT plants (Figure 7g–m). In the cross-section, the *zmd1* mutants showed increases in stalk cell length and the number of vascular bundles but no changes in width (Figure 7h–n). These results confirmed our findings that genes identified in the green module were positively associated with internode length, weight, and diameter as predicted by our WGCN analysis.

In addition to the stalk, the loss of the *ZmD1* function also influenced leaf development and grain yield (Figure 8). The *zmd1* mutants did not show any difference in leaf number and leaf angle (Figure 8a–c). However, *ZmD1* mutation decreased the leaf cell length and increased cell number, but did not change the leaf cell width (Figure 8d–i). Moreover, the tassel length, tassel branch number, and days to anthesis were noticeably diminished in the *zmd1* mutants compared to the WT (Figure 8j–m). In addition,

the seed length, width, and hundred-grain weight were slightly reduced in *zmd1* mutants (Figure 8n–q).

Transcriptome analysis of *ZmD1*-regulated stalk development by RNA-sequencing

To investigate the role of *ZmD1* in regulating stalk development, we performed an RNA-Seq analysis of *ZmD1* mutant and WT stalks. FPKM values for all 39 495 genes in maize were employed to construct a Pearson's distance correlation matrix to compare *ZmD1* mutant and WT transcriptomes. The heatmap distinguished the *ZmD1* and WT groups, and the three biological replicates of each sample were highly correlated (Figure 9a,b). We identified 760 upregulated and 274 downregulated DEGs (Table S9) (log2-fold change ≥1 and FDR <5%) (Figure 9c). Moreover, the GO analysis indicated that these DEGs were involved in metabolic processes, cellular component organization or biogenesis, and developmental processes (Figure 9d). The *zmd1* mutation increased the expression of cell size-related genes and decreased that of genes relevant to plant hormone signal transduction (Figure 9e–h). Q-PCR was employed to confirm gene expression in *zmd1* mutant and WT plants, including hormone-related genes *Zm00001d027900*, *Zm00001d020614*, *Zm00001d022530*, *Zm00001d029558*, *Zm00001d005813*, and *Zm00001d029448* (Figure 9f), cell size-related genes *Zm00001d019552*, *Zm00001d053998*, *Zm00001d002899* (*px18*), and *Zm00001d052103* (Figure 9h). Moreover, the gene expression of *ZmBZR1* was upregulated in the *zmd1* mutant, as predicted by our analysis that the expression trends of *ZmD1* and *ZmBZR1* were complementary in maize stalks (Figure 9h).

Interestingly, approximately 37.9% (392/1034) and 31.1% (322/1034) of *ZmD1*-regulated DEGs overlapped with the elongation genes (MS_N7 vs. ES_N7) and the division genes (ES_Top vs. ES_N1), respectively (Figure 9i). Twenty-four of the 392 DEGs were TFs, including bHLH, bZIP, ERF, TEOSINTE BRANCHED 1 (TCP), and HSF family genes, which were mainly involved in growth and development and response to stress (Figure 9j). TCP (*TCPTF16* and *TCPTF25*) and bZIP (*bZIP53*, *bZIP89*, and *bZIP117*) family genes showed significantly upregulated expression patterns in *zmd1* mutants (Figure 9j). The *bZIP53* gene participates in the regulation of plant growth by responding to the gibberellin signalling pathway (Lv *et al.*, 2021). Several TCP family genes regulate the aspects of cell elongation and division (Danisman, 2016).

In summary, the *ZmD1* gene regulated stalk development by influencing cell length and width, which demonstrates the predictive power of our WGCN data and suggests that the key modules and hub genes may function to determine stalk length and strength in maize.

Figure 5 Coexpression network analysis of RNA-seq of the maize stalk at the elongation stage and identification of critical genes predicting internode development. (a) Scale independence and mean connectivity of the network at different soft-threshold powers. The left panel displays the correlation of the soft threshold with the scale-free fit index. The right panel displays the influence of soft-threshold power on mean connectivity. (b) Hierarchical cluster tree showing coexpression modules identified by WGCNA. Each 'leaf' (short vertical line) corresponds to an individual gene. The major tree branches constitute 25 modules labelled with different colours. (c) Module-phenotype association. Each row corresponds to a coloured module. The number of genes is indicated in the coloured box of each module. Each column corresponds to a phenotype. The correlation coefficient between the module and trait is indicated in red colour for positive correlations (ranging from 0 to 1) and in blue for negative correlations (ranging from 0 to −1), while the numbers within each coloured box give the *P* values for the statistical significance of each correlation. (d) Scatter plot showing the correlations between genes in the green module and phenotypes, including length, weight, diameter, and perimeter of every internode. (e) Heatmap showing the expression profile of all the coexpressed genes in the green module. The colour scale represents the *Z* score. Bar graphs show the consensus expression pattern of the coexpressed genes in this green module. (f) Functional category enrichment of the genes in the green module.

(a)

(b)

(c)

(d)

(e)

(f)

(a)

(b)

(c)

(d)

(e)
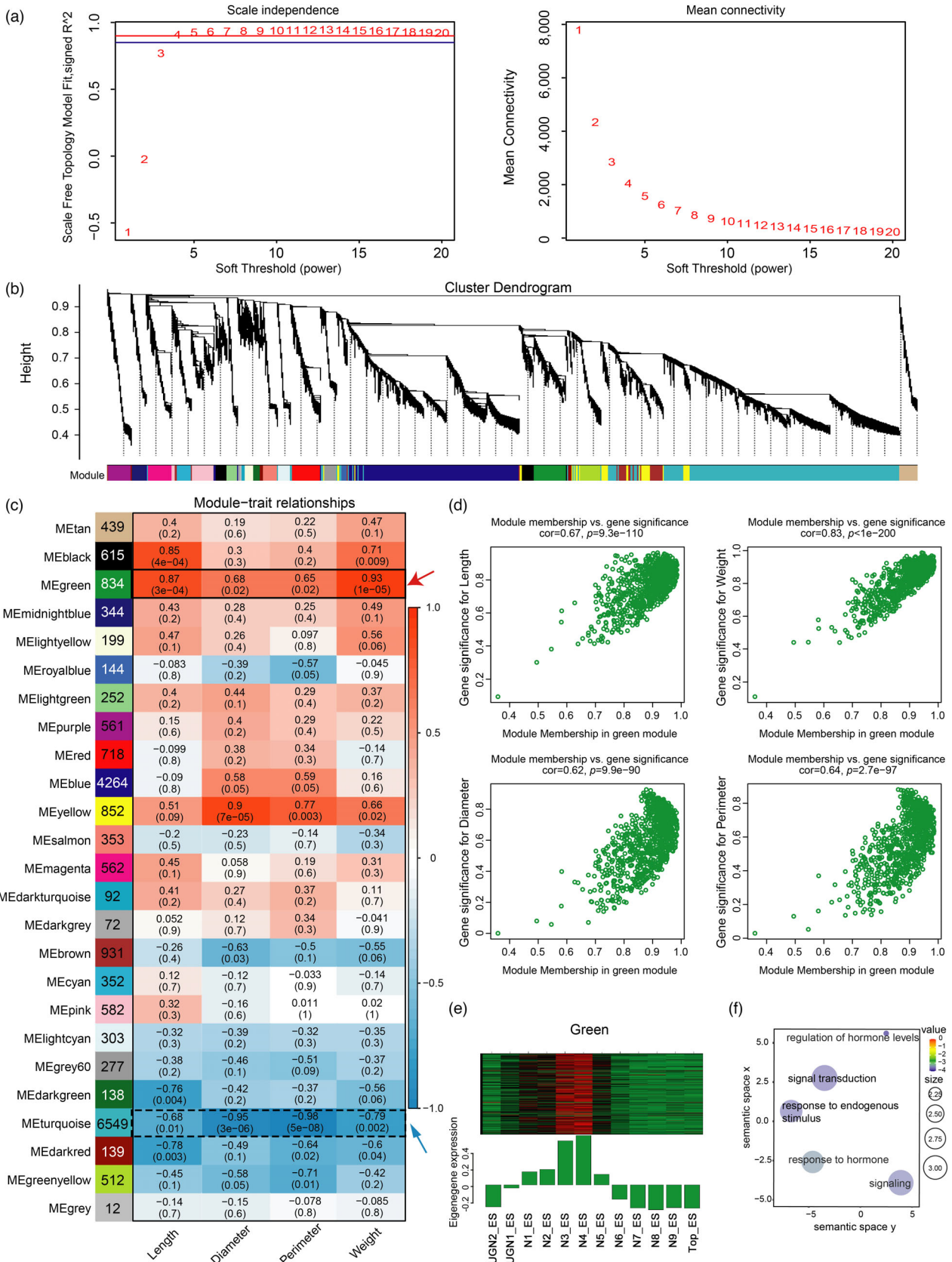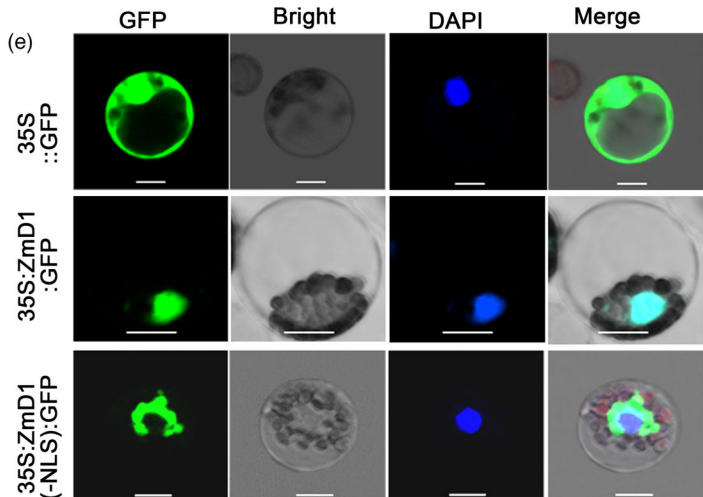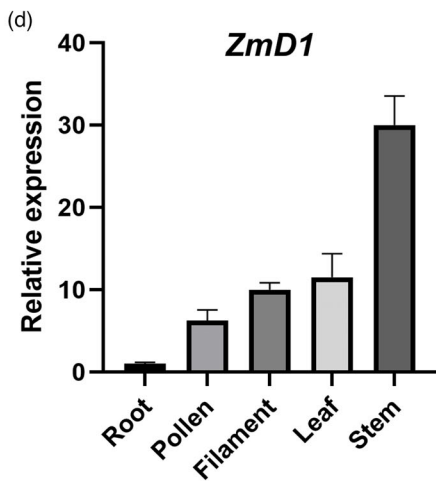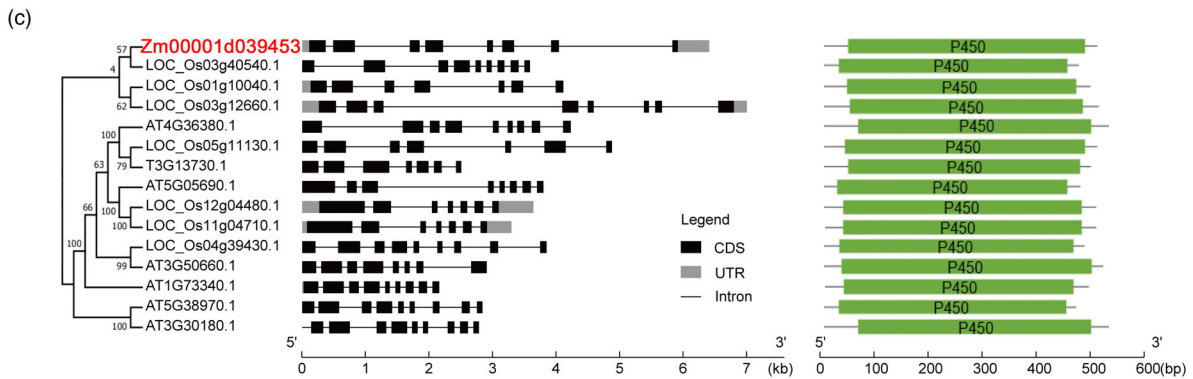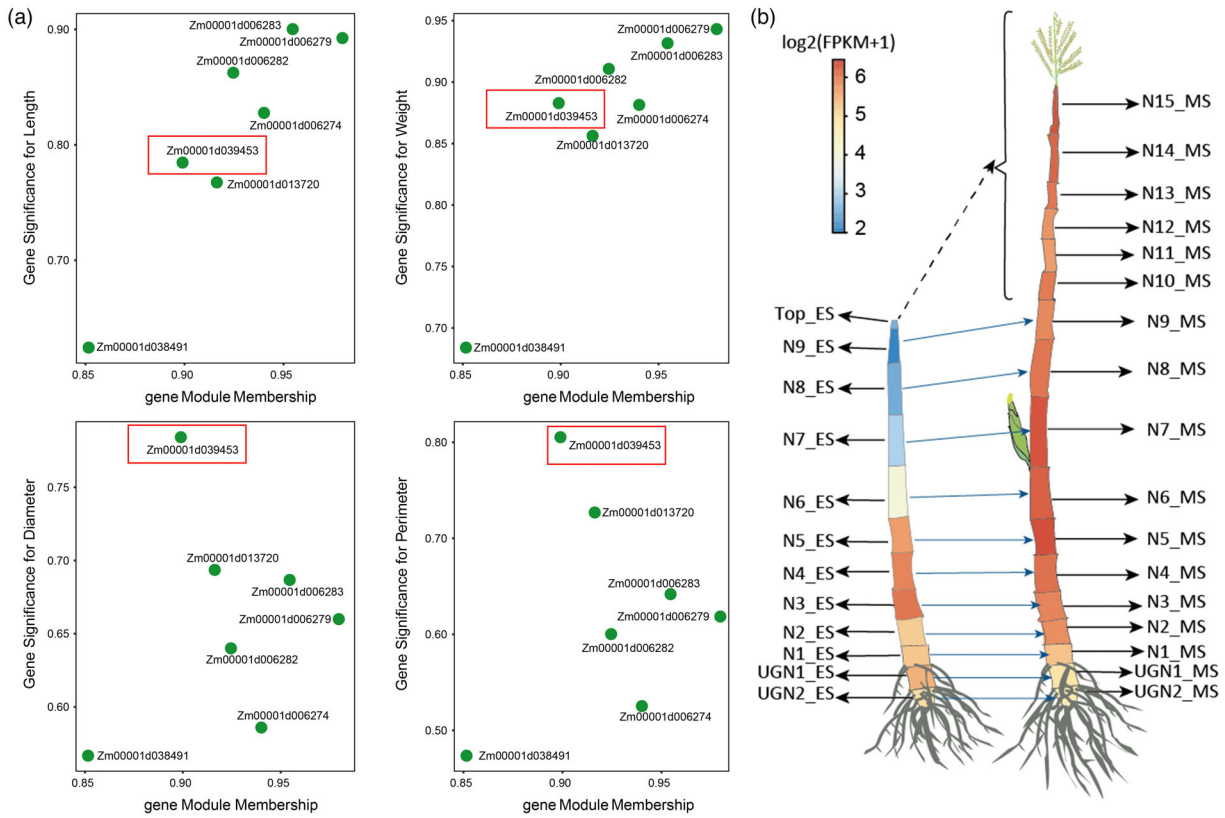
Figure 6 Expression pattern of the candidate gene *Zm00001d039453* (*ZmD1*) in maize stalks. (a) The correlations of genes involved in the regulation of hormone levels and phenotypes (length, weight, diameter, and perimeter) are shown. (b) The expression pattern of *ZmD1* in individual internodes of maize stalks at two stages. (c) Phylogenetic tree, gene structure, and protein domains of ZmD1 proteins among *Arabidopsis*, rice, and maize. The phylogenetic tree was constructed with MEGA7 using the full-length amino acid sequences. The yellow exons code a P450 domain. (d) The expression level of *ZmD1* in different maize tissues. (e) The nuclear-location pattern of ZmD1 in maize protoplasts in the absence or presence of nuclear-location signal (NLS) peptide. Scale bars = 10 μm.

Discussion

In this study, we constructed a dynamic, spatiotemporally resolved transcriptome landscape of all internodes of maize stalks at the fast ES and MS to identify new specific regulators during maize development. Although several transcriptional profiles of the specific internodes have been generated (Hoopes *et al.*, 2019; Stelpflug *et al.*, 2016; Wang *et al.*, 2020), little is known about the transcriptional dynamics in the whole maize stalk at the rapid ES and MS, which play important roles in final PH and stalk strength. The transcriptome dataset is of high quality, and the results of biological replicates are very reproducible. This is the first whole RNA-seq transcriptome dataset to characterize and utilize the developmental internodes within elongating and maturation stalks of maize.

The dynamic transcriptome data clearly highlighted four distinct zones within the whole stalks at ES and MS, including the elongation partially complete, division, base, and mature zones (Bleecker *et al.*, 1986; Wei *et al.*, 2019). We identified 13 964 genes with a high CV and classified them into nine

coexpression clusters according to their expression patterns. This large collection of gene clusters provides a valuable and credible resource for crop improvement, which will substantially enhance our understanding of the genetic mechanisms of maize stalk development. For example, we identified plant growth-related genes reported previously with a specific expression pattern at the ES or MS, such as *Zm Hexosyltransferase*, *ZmBzip28*, and *ZmD1* in Zone I; *ZmRPH1*, *ZmACS7*, and *ZmLox10* in Zone II; and *ZmUB2*, *ZmUB3* and *ZmTSH4* in Zone IV (Figure 1d–g) (Che *et al.*, 2010; Christensen *et al.*, 2013; Chuck *et al.*, 2014; Kim *et al.*, 2005; Li *et al.*, 2020a,b; Peng *et al.*, 2019). Furthermore, the dynamic transcriptome implied numerous TFs and hormonal response genes essential for stalk elongation and growth in maize. These gene resources could be used in maize genetic breeding for PH improvement. Our dataset also provided the phenotype relationship with targeted genes for stalk development. It will be of interest to determine and explore how these genes play key roles at specific target genes to mediate stalk development in maize. In addition to the potential roles of candidate genes in influencing PH, the combination of technical innovation such as synthetic
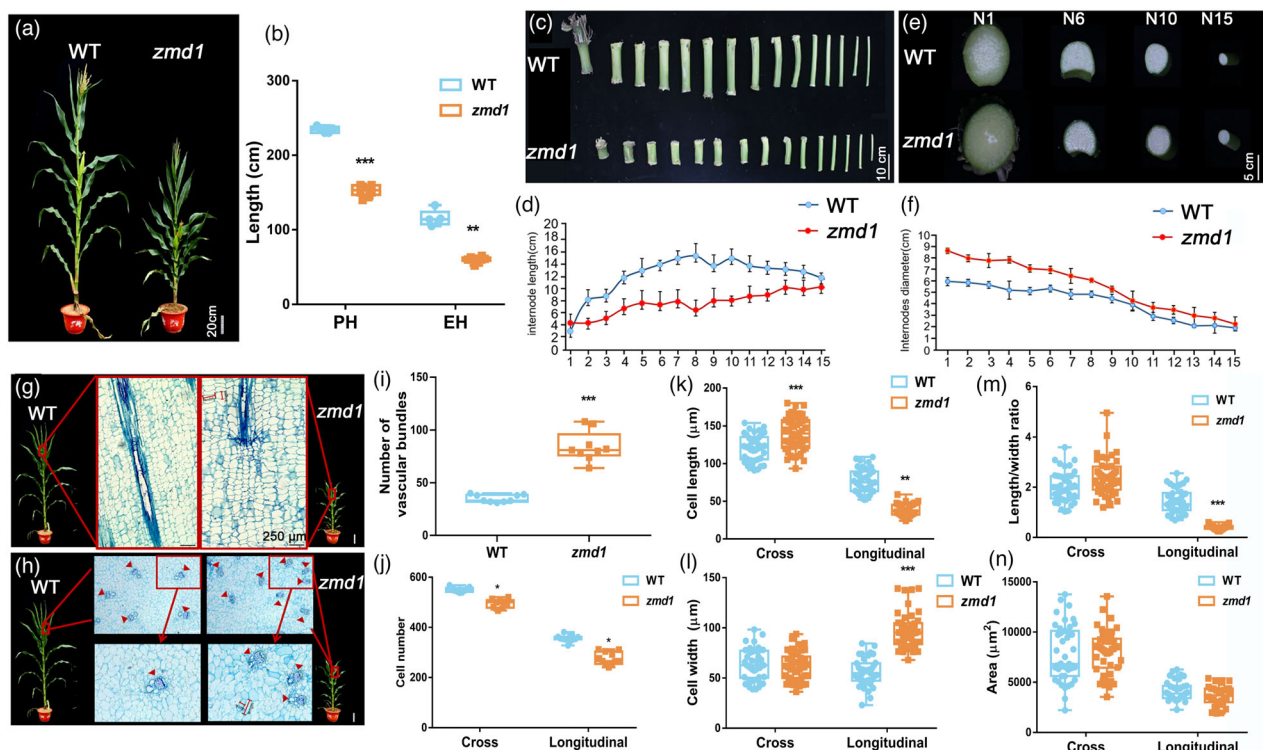
Figure 7 Role of *ZmD1* in regulating stalk development in maize. (a, b) Phenotype plant height (PH) and ear height (EH) of *zmd1* mutant and wild type (WT) maize plants at the mature stage (*N* = 20). (c–f) The internode morphology and length of the *zmd1* mutant and WT plants in the longitudinal section (c, d) and the cross-section (e, f). (g, h) Cell phenotypes of mutant and WT stalks in longitudinal (g) and cross-sections (h). Bar = 250 μm. (i–n). The number of vascular bundles (i), stalk cell number (j), length (k), width (l), length/width ratio (m), and area (n) in the cross and longitudinal section. **P* < 0.05; ***P* < 0.01; ****P* < 0.001 compared with WT.
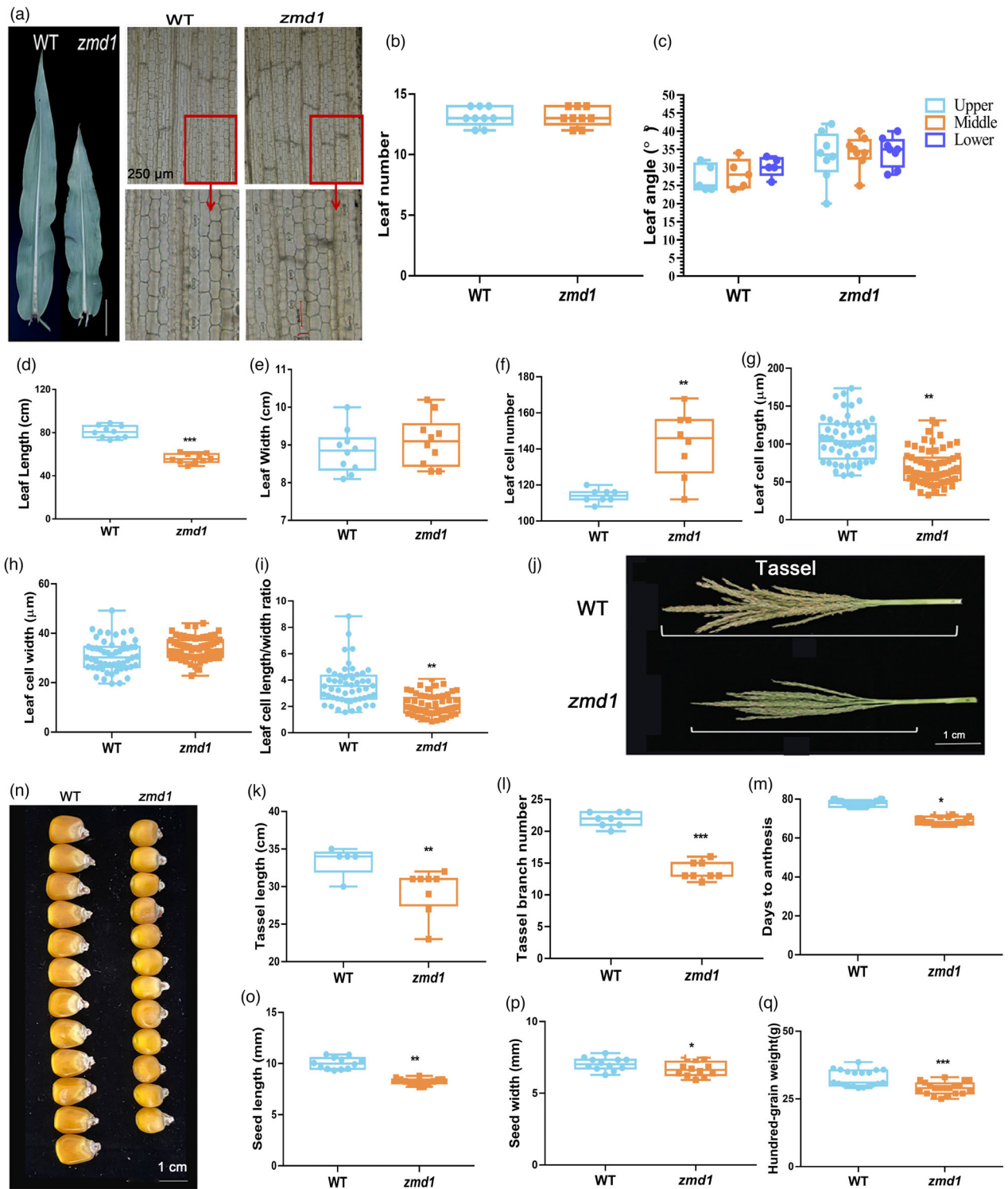
Figure 8 Role of *ZmD1* in regulating leaf, tassel, and seed development in maize. (a) Morphology of the ear leaves in mature maize. (b–e) Ear leaf number (b), angle (c), length (d), and width (e) in mature maize were statistically analysed. (f–i) Cell number (f), cell length (g), cell width (h), and length/width ratio of ear leaf (i). (j–l) Tassel phenotype (j), tassel length (k), and branch number (l) of normal compared with *zmd1* mutants. (m) Variations in days to anthesis. (n–q) Kernel morphology (n), length (o), width (p), and grain weight of hundred kernels (q) between *zmd1* and WT. *$P < 0.05$; **$P < 0.01$; ***$P < 0.001$ compared with WT.

biology and genome editing will allow greater control of plant architecture for crop improvement in future agriculture.

For better resistance to lodging, short but thick stature is an ideal agronomic trait of stalks. Both stalk length and width are regulated by stem elongation driven by cell division and cell expansion within the internodes. Although *dwarf* and *semidwarf* mutants have been widely used in rice (e.g., *sd1* gene) and wheat (e.g., *Rht* gene) breeding, many GA biosynthesis/
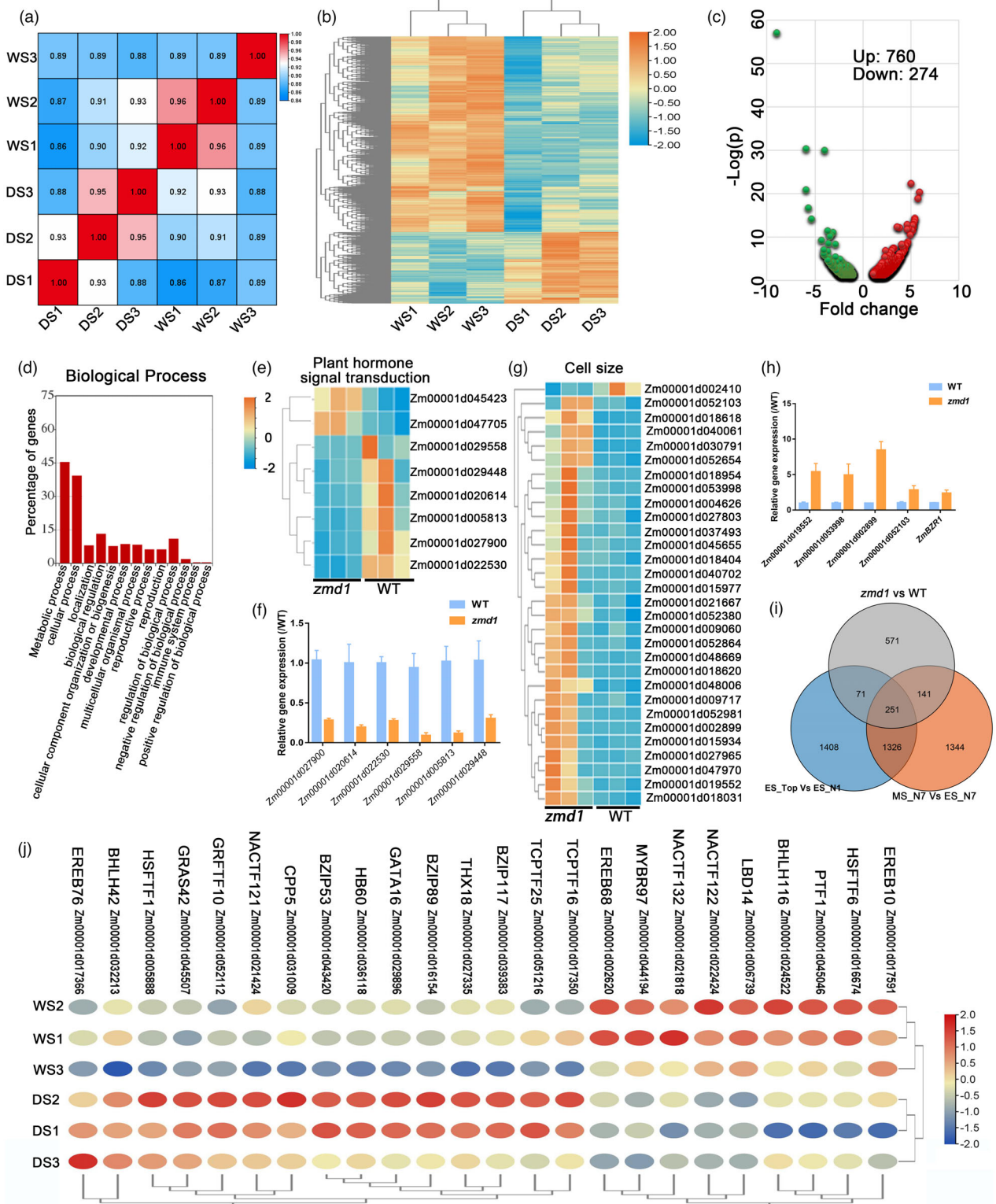
Figure 9 Transcriptome analysis of *ZmD1*-regulated differentially expressed genes (DEGs). (a) Pearson's correlation analysis of the gene expression between *ZmD1* mutants and WT. WS: WT stalk; DS, *ZmD1* stalk. (b) A total of 1034 DEGs of *zmd1* mutant stalks compared with WT stalks. (c) Volcano plots showing the number of DEGs regulated by ZmD1. (d) Functional enrichment of *zmd1*/WT-specific DEGs. (e–h) Heatmaps showing the genes involved in the regulation of plant hormone transduction (e) and cell size (g). Quantitative PCR results of selected genes involved in the regulation of plant hormone transduction (f) and cell size (h). (i) Venn diagram showing the distribution of unique and common DEGs among *zmd1* vs. WT, ES_Top vs. ES_N1, and MS_N7 vs. ES_N7. (j) Heatmap showing the 24 common transcription factors regulated by *ZmD1*, cell division and elongation.

signalling deficient maize mutants are detrimental to yield (Chen *et al*., 2014; Lawit *et al*., 2010; Sasaki *et al*., 2002). Thus, identifying new regulators that directly regulate cell division and expansion is a matter of great urgency. Combining WGCNA with the stalk phenotyping (internode length, weight, diameter, and perimeter), we identified the green module, which was positively correlated with length and weight and the turquoise module, which showed a strong negative correlation with diameter and perimeter (Figure 5c). The green module contained 2 BR-related genes (*ZmCYP87A2 and ZmD1*) and 4 auxin-related genes, which were previously shown to control plant growth and development (Guo *et al*., 2021; Kim *et al*., 2005).

It has been reported that BRs play a crucial role in determining stalk elongation and expansion. In maize, the extreme *dwarf* phenotype was associated with several BR mutants, such as *na2 (ZmDWF1)*, *na1 (Zmdet2)*, and *brd1 (Zmbrd1)* (Castorina *et al*., 2018; Knoch *et al*., 2018; Makarevitch *et al*., 2012). In *Arabidopsis thaliana*, *Cyp90D1*, the ortholog of *ZmD1*, encodes a cytochrome P-450 gene that was shown to catalyse the C-23 hydroxylation of several BRs (the enzyme has a broad specificity for 22-hydroxylated substrates) (Kim *et al*., 2005; Ohnishi *et al*., 2012). In plants, the CYP90 family gene was directly targeted by *BZR1*, which is a BR-related TF negatively correlated with cell and fruit size (Su *et al*., 2021). Interestingly, *ZmBZR1* was included in the turquoise module and was negatively correlated with internode length and weight (Figure S4). Moreover, the expression trends of *ZmD1* and *ZmBZR1* were complementary in maize stalks, suggesting a possible hormone pathway for the regulation of stalk development in maize.

However, the function of *BZR1* in PH is controversial because many studies have shown that cell elongation is severely suppressed in most BR-deficient and BR-insensitive mutants (Nolan *et al*., 2017; Zhang *et al*., 2014a). Our previous study also indicated that overexpression of *ZmBZR1* in transgenic *Arabidopsis* plants leads to a significant increase in plant size (Zhang *et al*., 2020). Most recently, *ZmBES1/BZR1-5* was shown to positively regulate kernel size by interacting with casein kinase II subunit β4 (*ZmCKIIβ4*) and ferredoxin 2 (*ZmFdx2*) (Sun *et al*., 2021). *BZR1* is a transcriptional repressor with dual roles in BR homeostasis and growth responses via the direct binding of the promoter of effector or feedback-regulated BR biosynthetic genes (Wang *et al*., 2002). The dominant *bzr1-1D* mutation causes insensitivity to the BR biosynthetic inhibitor by suppressing the BR-insensitive *bri1* and *bin2* mutants, indicating a positive role for *BZR1* in BR signalling. However, *BZR1* can promote feedback inhibition of BR biosynthesis by acting as a negative regulator of BR-regulated growth (He *et al*., 2005). In this study, we directly focused on the function of *ZmD1*, a possible effector of *BZR1* (Su *et al*., 2021).The *ZmD1* gene mutant generated by CRISPR/Cas9 technology exhibits many effects on morphological and physiological phenotypes in maize, including lowering PH and ear height, enlarging the leaf angle, advancing flowering time, and thickening the internode, which corresponds to the ideal plant architecture (Figure 7). These results validate the predictive power of our transcriptome data and provide key modules and hub genes that aid in the elucidation of the pathways and processes governing stalk length and strength.

In summary, our results revealed a previously undescribed global transcriptome and coexpression network regulating stalk development in maize with a striking feature of dynamic changes in transcript profiles from the ES to MS. The candidate modules and genes identified herein provide a valuable resource for ideal plant architecture breeding in maize.

Experimental procedures

Plant material and sample collection

All the mutant and inbred lines of maize were planted in the experimental field in Langfang, Hebei Province, China, during the summer and in Ledong, Hainan Province, China, during the winter. Internode samples from the inbred line B73 were taken at the ES and MS for RNA extraction and transcriptome analysis. The internodes under the aerial root were considered underground internodes, and the other internodes were numbered from the bottom to the top. Samples of the root, pollen, filament, and leaf stem were also taken. Three biological replicates were collected for every sample. Wilcox tests were used to determine the significance of differences between pairs of samples.

Transgene constructs and targeted gene editing

CRISPR/Cas9 technology was used to generate *zmd1* knockout plants, and single-guide RNA sequences (listed in Table S8) were cloned into pCPB-UBi::hspCas9 (a gift from Prof. Haiyang Wang). The WT maize inbred line used for a mutant generation was ZC01, a private receptor inbred line created by the China National Seed Group Co., Ltd (Wuhan, China). These mutants were confirmed using PCR with primers (listed in Table S8) and direct sequencing.

Trait measurements

All morphological traits were measured in the field at the ES and the MS, and the histological traits were measured after cutting the sample into slices. PH, leaf length, tassel length, leaf width, node length, node weight, node diameter, node perimeter, stalk cell length, and stalk cell width were recorded.

High-throughput RNA-seq and data analysis

Total RNA was extracted from each sample using the RNeasy Plus Mini Kit (Vazyme Biotech, Beijing, China), and cDNA libraries were generated using the NEBNext Ultra RNA Library Prep Kit (NEB). The quantified libraries were prepared for sequencing on the Illumina HiSeq X-ten sequencing platform. The raw data after removing adaptors and low-quality reads ($Q < 20$) were aligned to the maize reference genome (v4) using HISAT2 (Kim *et al*., 2019), and gene expression levels were calculated by featureCounts (Liao *et al*., 2014) using default parameters and then converted to FPKM values.

Gene clustering

Genes detected for the two stages were filtered with a CV cutoff (>0.4) and grouped into various clusters using the Mfuzz package with the fuzzy c-means algorithm (Kumar and Futschik, 2007) in R software v3.6.1.

Coexpression network construction

Weighted gene coexpression network analysis was performed for 12 internode samples at the ES with the WGCNA package (Langfelder and Horvath, 2008) in R v3.6.1. These genes were filtered with a cutoff (CV > 0.4), and then WGCNA was performed to calculate the topological overlap matrix from a

pairwise correlation-based adjacency matrix. The neighbourhood similarity among genes was calculated, and the gene coexpression modules were identified by average linkage hierarchical clustering. A total of 25 modules were identified using the dynamic hybrid tree cut algorithm and minimum module size of 30 genes. The networks were visualized with Cytoscape v3.6.1 (http://cytoscape.org/).

Functional enrichment analysis

GO enrichment analysis of cluster genes and module genes was performed using the agriGO v2.0 database with the Fisher's test and the multitest adjustment method of Yekutieli (FDR under dependency) (Tian *et al.*, 2017). The terms with a cutoff false detection rate (FDR) of <0.05 were considered significantly enriched. The top 20 biological process terms were visualized using the REVIGO database (http://revigo.irb.hr/) with default parameters to reduce the GO dimension.

Phylogenetic tree analysis

The phylogenetic relationships of the ZmD1 protein families from *Zea mays*, *Oryza sativa*, and *A. thaliana* were inferred. Accessions were acquired through BLASTP of the NCBI using the ZmD1 proteins. Protein sequence alignment was performed with default parameters, and then, the resulting sequence was subjected to the maximum likelihood method PhyML to generate a phylogenetic tree in MEGA v7.0 (Kumar *et al.*, 2016).

Subcellular localization

The full-length cDNA of *ZmD1* was cloned and transferred into the pRTL2 vector to express the ZmD1-GFP fusion protein at the *N*-terminus of green fluorescent protein (GFP). The fusion construct (*35S::ZmD1-GFP*), control construct (*35S::GFP*), and ZmD1 loss nuclear localization sequence (NLS) construct (*35S::ZmD1(-NLS)-GFP*) were transformed into maize protoplasts. Confocal microscopy (ZEISS, LSM88) was used to detect fluorescence after culture for 16 h.

qPCR validation

Total RNA was extracted using the RNeasy Plus Mini Kit (Vazyme Biotech, Beijing, China). First-strand cDNA was synthesized and employed as a template for qPCR performed with real-time qPCR Master Mix (RR430A; Takara, Shiga, Japan). Actin was used to normalize relative expression levels. All primers are listed in Table S4.

Conflict of interests

The authors declare no conflicts of interest.

Author contributions

L.P. and C.Z. conceived and designed the experiments. All authors performed the experiments and analysed data. L.L., W.G., and L.P. wrote the paper. All authors read and approved the manuscript.

Data availability statement

The raw RNA-seq data are available at the NGDC GSA accession number CRA005188 at the following URL: https://bigd.big.ac.cn/gsa/browse/CRA005188.

References

Avila, L.M., Cerrudo, D., Swanton, C. and Lukens, L. (2016) Brevis plant1, a putative inositol polyphosphate 5-phosphatase, is required for internode elongation in maize. *J. Exp. Bot.* **67**, 1577–1588.

Bleecker, A.B., Schuette, J.L. and Kende, H. (1986) Anatomical analysis of growth and developmental patterns in the internode of deepwater rice. *Planta*, **169**, 490–497.

Brugiere, N., Jiao, S., Hantke, S., Zinselmeier, C., Roessler, J.A., Niu, X., Jones, R.J. *et al.* (2003) Cytokinin oxidase gene expression in maize is localized to the vasculature, and is induced by cytokinins, abscisic acid, and abiotic stress. *Plant Physiol.* **132**, 1228–1240.

Cassani, E., Bertolini, E., Cerino Badone, F., Landoni, M., Gavina, D., Sirizzotti, A. and Pilu, R. (2009) Characterization of the first dominant dwarf maize mutant carrying a single amino acid insertion in the VHYNP domain of the dwarf8 gene. *Mol. Breed.* **24**, 375–385.

Castorina, G., Persico, M., Zilio, M., Sangiorgio, S., Carabelli, L. and Consonni, G. (2018) The maize lilliputian1 (lil1) gene, encoding a brassinosteroid cytochrome P450 C-6 oxidase, is involved in plant growth and drought response. *Ann. Bot.* **122**, 227–238.

Che, P., Bussell, J.D., Zhou, W., Estavillo, G.M., Pogson, B.J. and Smith, S.M. (2010) Signaling from the endoplasmic reticulum activates brassinosteroid signaling and promotes acclimation to stress in Arabidopsis. *Sci. Signal.* **3**, ra69.

Chen, Y., Fan, X., Song, W., Zhang, Y. and Xu, G. (2012) Over-expression of OsPIN2 leads to increased tiller numbers, angle and shorter plant height through suppression of OsLAZY1. *Plant Biotechnol. J.* **10**, 139–149.

Chen, Y., Hou, M., Liu, L., Wu, S., Shen, Y., Ishiyama, K., Kobayashi, M. *et al.* (2014) The maize DWARF1 encodes a gibberellin 3-oxidase and is dual localized to the nucleus and cytosol. *Plant Physiol.* **166**, 2028–2039.

Choe, S., Noguchi, T., Fujioka, S., Takatsuto, S., Tissier, C.P., Gregory, B.D., Ross, A.S. *et al.* (1999) The Arabidopsis dwf7/ste1 mutant is defective in the delta7 sterol C-5 desaturation step leading to brassinosteroid biosynthesis. *Plant Cell*, **11**, 207–221.

Christensen, S.A., Nemchenko, A., Borrego, E., Murray, I., Sobhy, I.S., Bosak, L., DeBlasio, S. *et al.* (2013) The maize lipoxygenase, ZmLOX10, mediates green leaf volatile, jasmonate and herbivore-induced plant volatile production for defense against insect attack. *Plant J.* **74**, 59–73.

Chuck, G., Whipple, C., Jackson, D. and Hake, S. (2010) The maize SBP-box transcription factor encoded by tasselsheath4 regulates bract development and the establishment of meristem boundaries. *Development*, **137**, 1243–1250.

Chuck, G.S., Brown, P.J., Meeley, R. and Hake, S. (2014) Maize SBP-box transcription factors unbranched2 and unbranched3 affect yield traits by regulating the rate of lateral primordia initiation. *Proc. Natl. Acad. Sci. USA*, **111**, 18775–18780.

Cui, K., He, C.Y., Zhang, J.G., Duan, A.G. and Zeng, Y.F. (2012) Temporal and spatial profiling of internode elongation-associated protein expression in rapidly growing culms of bamboo. *J. Proteome Res.* **11**, 2492–2507.

Danisman, S. (2016) TCP transcription factors at the interface between environmental challenges and the plant's growth responses. *Front. Plant Sci.* **7**, 1930.

Fournier, C. and Andrieu, B. (2000) Dynamics of the elongation of internodes in maize (*Zea mays* L.). Effects of shade treatment on elongation patterns. *Ann. Bot.-London*, **86**, 1127–1134.

Guo, F., Huang, Y., Qi, P., Lian, G., Hu, X., Han, N., Wang, J. et al. (2021) Functional analysis of auxin receptor OsTIR1/OsAFB family members in rice grain yield, tillering, plant height, root system, germination, and auxinic herbicide resistance. *New Phytol.* **229**, 2676–2692.

He, J.X., Gendron, J.M., Sun, Y., Gampala, S.S., Gendron, N., Sun, C.Q. and Wang, Z.Y. (2005) BZR1 is a transcriptional repressor with dual roles in brassinosteroid homeostasis and growth responses. *Science*, **307**, 1634–1638.

Hoopes, G.M., Hamilton, J.P., Wood, J.C., Esteban, E., Pasha, A., Vaillancourt, B., Provart, N.J. et al. (2019) An updated gene atlas for maize reveals organ-specific and stress-induced genes. *Plant J.* **97**, 1154–1167.

Jiao, S., Hazebroek, J.P., Chamberlin, M.A., Perkins, M., Sandhu, A.S., Gupta, R., Simcox, K.D. et al. (2019) Chitinase-like1 plays a role in stalk tensile strength in maize. *Plant Physiol.* **181**, 1127–1147.

Kashiwagi, T., Madoka, Y., Hirotsu, N. and Ishimaru, K. (2006) Locus prl5 improves lodging resistance of rice by delaying senescence and increasing carbohydrate reaccumulation. *Plant Physiol. Biochem.* **44**, 152–157.

Kim, D., Paggi, J.M., Park, C., Bennett, C. and Salzberg, S.L. (2019) Graph-based genome alignment and genotyping with HISAT2 and HISAT-genotype. *Nat. Biotechnol.* **37**, 907–915.

Kim, G.T., Fujioka, S., Kozuka, T., Tax, F.E., Takatsuto, S., Yoshida, S. and Tsukaya, H. (2005) CYP90C1 and CYP90D1 are involved in different steps in the brassinosteroid biosynthesis pathway in Arabidopsis thaliana. *Plant J.* **41**, 710–721.

Kim, J.H. and Lee, B.H. (2006) GROWTH-REGULATING FACTOR4 of Arabidopsis thaliana is required for development of leaves, cotyledons, and shoot apical meristem. *J. Plant Biol.* **49**, 463–468.

Knoch, E., Sugawara, S., Mori, T., Poulsen, C., Fukushima, A., Harholt, J., Fujimoto, Y. et al. (2018) Third DWF1 paralog in Solanaceae, sterol Delta(24)-isomerase, branches withanolide biosynthesis from the general phytosterol pathway. *Proc. Natl. Acad. Sci. USA*, **115**, E8096–E8103.

Ku, L.X., Zhang, J., Guo, S.L., Liu, H.Y., Zhao, R.F. and Chen, Y.H. (2012) Integrated multiple population analysis of leaf architecture traits in maize (Zea mays L.). *J. Exp. Bot.* **63**, 261–274.

Kumar, L., Futschik, E. and Mfuzz, M. (2007) A software package for soft clustering of microarray data. *Bioinformation*, **20**, 5–7.

Kumar, S., Stecher, G. and Tamura, K. (2016) MEGA7: Molecular evolutionary genetics analysis version 7.0 for bigger datasets. *Mol. Biol. Evol.* **33**, 1870–1874.

Langfelder, P. and Horvath, S. (2008) WGCNA: an R package for weighted correlation network analysis. *BMC Bioinform.* **9**, 559.

Lawit, S.J., Wych, H.M., Xu, D.P., Kundu, S. and Tomes, D.T. (2010) Maize DELLA proteins dwarf plant8 and dwarf plant9 as modulators of plant development. *Plant Cell Physiol.* **51**, 1854–1868.

Li, G., Wang, D., Yang, R., Logan, K., Chen, H., Zhang, S., Skaggs, M.I. et al. (2014) Temporal patterns of gene expression in developing maize endosperm identified through transcriptome sequencing. *Proc. Natl. Acad. Sci. USA*, **111**, 7582–7587.

Li, H., Wang, L., Liu, M., Dong, Z., Li, Q., Fei, S., Xiang, H. et al. (2020a) Maize plant architecture is regulated by the ethylene biosynthetic gene ZmACS7. *Plant Physiol.* **183**, 1184–1199.

Li, W., Ge, F., Qiang, Z., Zhu, L., Zhang, S., Chen, L., Wang, X. et al. (2020b) Maize ZmRPH1 encodes a microtubule-associated protein that controls plant and ear height. *Plant Biotechnol. J.* **18**, 1345–1347.

Liao, Y., Smyth, G.K. and Shi, W. (2014) featureCounts: an efficient general purpose program for assigning sequence reads to genomic features. *Bioinformatics*, **30**, 923–930.

Liu, N., Zhao, Y.J., Wu, J.W., Wei, Y.M., Ren, R.C., Zang, J., Zhang, W.T. et al. (2020) Overexpression of ZmDWF4 improves major agronomic traits and enhances yield in maize. *Mol. Breed.* **40**, 71.

Lu, S., Li, M., Zhang, M., Lu, M., Wan, X.Q., Wang, P.W. and Liu, W.G. (2020) Genome-wide association study of plant and ear height in maize. *Trop. Plant Biol.* **13**, 262–273.

Lv, H., Li, X., Li, H., Hu, Y., Liu, H., Wen, S., Li, Y. et al. (2021) Gibberellin induced transcription factor bZIP53 regulates CesA1 expression in maize kernels. *PLoS One*, **16**, e0244591.

Ma, C.L., Guo, J., Kang, Y., Doman, K., Bryan, A.C., Tax, F.E., Yamaguchi, Y. et al. (2014) AtPEPTIDE RECEPTOR2 mediates the AtPEPTIDE1-induced

cytosolic Ca2+ rise, which is required for the suppression of Glutamine Dumper gene expression in Arabidopsis roots. *J. Integr. Plant Biol.* **56**, 684–694.

Makarevitch, I., Thompson, A., Muehlbauer, G.J. and Springer, N.M. (2012) Brd1 gene in maize encodes a brassinosteroid C-6 oxidase. *PLoS One*, **7**, e30798.

Mei, X., Nan, J., Zhao, Z., Yao, S., Wang, W., Yang, Y., Bai, Y. et al. (2021) Maize transcription factor ZmNF-YC13 regulates plant architecture. *J. Exp. Bot.* **72**, 4757–4772.

Nolan, T., Chen, J. and Yin, Y. (2017) Cross-talk of Brassinosteroid signaling in controlling growth and stress responses. *Biochem. J.* **474**, 2641–2661.

Ohnishi, T., Godza, B., Watanabe, B., Fujioka, S., Hategan, L., Ide, K., Shibata, K. et al. (2012) CYP90A1/CPD, a brassinosteroid biosynthetic cytochrome P450 of Arabidopsis, catalyzes C-3 oxidation. *J. Biol. Chem.* **287**, 31551–31560.

Peiffer, J.A., Flint-Garcia, S.A., De Leon, N., McMullen, M.D., Kaeppler, S.M. and Buckler, E.S. (2013) The genetic architecture of maize stalk strength. *Plos One*, **8**, e67066.

Peng, C., Wang, X., Feng, T., He, R., Zhang, M., Li, Z., Zhou, Y. et al. (2019) System analysis of MIRNAs in maize internode elongation. *Biomolecules*, **9**, 417.

Pratelli, R., Voll, L.M., Horst, R.J., Frommer, W.B. and Pilot, G. (2010) Stimulation of nonselective amino acid export by glutamine dumper proteins. *Plant Physiol.* **152**, 762–773.

Ren, Z.Z., Wu, L.C., Ku, L.X., Wang, H.T., Zeng, H.X., Su, H.H., Wei, L. et al. (2020) ZmILI1 regulates leaf angle by directly affecting liguleless1 expression in maize. *Plant Biotechnol. J.* **18**, 881–883.

Sasaki, A., Ashikari, M., Ueguchi-Tanaka, M., Itoh, H., Nishimura, A., Swapan, D., Ishiyama, K. et al. (2002) Green revolution: a mutant gibberellin-synthesis gene in rice. *Nature*, **416**, 701–702.

Stelpflug, S.C., Sekhon, R.S., Vaillancourt, B., Hirsch, C.N., Buell, C.R., de Leon, N. and Kaeppler, S.M. (2016) An expanded maize gene expression atlas based on rna sequencing and its use to explore root development. *Plant Genome*, **9**, 1–16.

Su, W., Shao, Z., Wang, M., Gan, X., Yang, X. and Lin, S. (2021) EjBZR1 represses fruit enlargement by binding to the EjCYP90 promoter in loquat. *Hortic Res.* **8**, 152.

Sun, F., Ding, L., Feng, W., Cao, Y., Lu, F., Yang, Q., Li, W. et al. (2021) Maize transcription factor ZmBES1/BZR1-5 positively regulates kernel size. *J. Exp. Bot.* **72**, 1714–1726.

Sun, Q., Liu, X., Yang, J., Liu, W., Du, Q., Wang, H., Fu, C. et al. (2018) MicroRNA528 affects lodging resistance of maize by regulating lignin biosynthesis under nitrogen-luxury conditions. *Mol. Plant*, **11**, 806–814.

Tang, W.Q., Deng, Z.P. and Wang, Z.Y. (2010) Proteomics shed light on the brassinosteroid signaling mechanisms. *Curr. Opin. Plant Biol.* **13**, 27–33.

Tian, T., Liu, Y., Yan, H., You, Q., Yi, X., Du, Z., Xu, W. et al. (2017) agriGO v2.0: a GO analysis toolkit for the agricultural community, 2017 update. *Nucleic Acids Res.* **45**, W122–W129.

Tran, T.M., McCubbin, T.J., Bihmidine, S., Julius, B.T., Baker, R.F., Schauflinger, M., Weil, C. et al. (2019) Maize carbohydrate partitioning defective33 encodes an MCTP protein and functions in sucrose export from leaves. *Mol. Plant*, **12**, 1278–1293.

Wang, X., Shi, Z., Zhang, R., Sun, X., Wang, J., Wang, S., Zhang, Y. et al. (2020) Stalk architecture, cell wall composition, and QTL underlying high stalk flexibility for improved lodging resistance in maize. *BMC Plant Biol.* **20**, 515.

Wang, Z.Y., Nakano, T., Gendron, J., He, J., Chen, M., Vafeados, D., Yang, Y. et al. (2002) Nuclear-localized BZR1 mediates brassinosteroid-induced growth and feedback suppression of brassinosteroid biosynthesis. *Dev. Cell*, **2**, 505–513.

Wei, Q., Guo, L., Jiao, C., Fei, Z., Chen, M., Cao, J., Ding, Y. et al. (2019) Characterization of the developmental dynamics of the elongation of a bamboo internode during the fast growth stage. *Tree Physiol.* **39**, 1201–1214.

Winkler, R.G. and Freeling, M. (1994) Physiological genetics of the dominant gibberellin-nonresponsive maize dwarfs, Dwarf8 and Dwarf9. *Planta*, **193**, 341–348.

Winkler, R.G. and Helentjaris, T. (1995) The maize Dwarf3 gene encodes a cytochrome P450-mediated early step in gibberellin biosynthesis. *Plant Cell*, **7**, 1307–1317.

Xiao, Y.J., Liu, H.J., Wu, L.J., Warburton, M. and Yan, J.B. (2017) Genome-wide association studies in maize: praise and stargaze. *Mol. Plant*, **10**, 359–374.

Yu, C.P., Chen, S.C., Chang, Y.M., Liu, W.Y., Lin, H.H., Lin, J.J., Chen, H.J. *et al.* (2015) Transcriptome dynamics of developing maize leaves and genomewide prediction of cis elements and their cognate transcription factors. *Proc. Natl. Acad. Sci. USA*, **112**, E2477–E2486.

Zhang, C., Bai, M.Y. and Chong, K. (2014a) Brassinosteroid-mediated regulation of agronomic traits in rice. *Plant Cell Rep.* **33**, 683–696.

Zhang, Q., Cheetamun, R., Dhugga, K.S., Rafalski, J.A., Tingey, S.V., Shirley, N.J., Taylor, J. *et al.* (2014b) Spatial gradients in cell wall composition and transcriptional profiles along elongating maize internodes. *BMC Plant Biol.* **14**, 27.

Zhang, X., Guo, W., Du, D., Pu, L. and Zhang, C. (2020) Overexpression of a maize BR transcription factor ZmBZR1 in Arabidopsis enlarges organ and seed size of the transgenic plants. *Plant Sci.* **292**, 110378.

Zhou, P., Hirsch, C.N., Briggs, S.P. and Springer, N.M. (2019) Dynamic patterns of gene expression additivity and regulatory variation throughout maize development. *Mol. Plant*, **12**, 410–425.

Zuber, U., Winzeler, H., Messmer, M.M., Keller, M., Keller, B., Schmid, J.E. and Stamp, P. (1999) Morphological traits associated with lodging resistance of spring wheat (*Triticum aestivum* L.). *J. Agron. Crop Sci.* **182**, 17–24.

Supporting information

Additional supporting information may be found online in the Supporting Information section at the end of the article.

Figure S1 Characterization of total gene expression and correlation analysis across all tissues.

Figure S2 Expression dynamics of TF families.

Figure S3 Functional enrichment of DEGs among five internodes.

Figure S4 The phenotype of maize internodes at the elongation stage and maturation stage.

Figure S5 Network connections of genes in the green modules.

Figure S6 The expression pattern of genes in the turquoise module.

Figure S7 The expression pattern of genes in the yellow module.

Figure S8 The expression correlation between *ZmD1* and *ZmBZR1*.

Figure S9 *zmd1* mutants were constructed by CRISPR-Cas9 technology.

Table S1 Gene expression and clusters of maize stalks at the ES and MS.

Table S2 Hormone-related gene expression of maize stalks at the ES and MS.

Table S3 The expression, numbers, and classes of all transcription factors of maize stalks at the ES and MS.

Table S4 List of differentially expressed genes (DEGs) between ES_Top and ES_N1.

Table S5 List of DEGs between MS_N7 and ES_N7.

Table S6 List of DEGs between MS_N1 and ES_N1.

Table S7 List of DEGs between MS_N7 and MS-N1.

Table S8 Guide RNA and specific maize gene primers used for real-time quantitative PCR.

Table S9 List of DEGs between *zmd1* and WT.